Autofocusing Using Multi-scale Local Correlation

Carole Nahum
ONERA, Chemin de la Hunière, 91761 PALAISEAU Cedex, France.
Phone: (33) 1 69 93 62 14, Fax: (33) 1 69 93 62 69, E-mail: nahum@onera.fr

ABSTRACT

Ground imaging using a Synthetic Aperture Radar (SAR) requires the knowledge of the antenna trajectory with a relative accuracy of a fraction of the wavelength upon an integration time of a few seconds.

This information is not always available from inertial navigation unit especially in the airborne framework and must be recovered from the radar signal itself using the techniques known as "autofocus".

We describe in this paper an original method designed at ONERA for the registration of looks. We show how it applies to autofocusing. It improves the map-drift algorithm making it time variant thus allowing for the correction of low frequency trajectory errors, and not only velocity bias.

Keywords : SAR – Look – Autofocus – Registration

1. INTRODUCTION

Ground imaging from a Synthetic Aperture Radar (SAR) requires the knowledge of the antenna trajectory with a relative accuracy of a fraction of wavelength upon an integration time of a few seconds. Whereas this is easily achieved in the satellite remote sensing framework, because of the high regularity of satellite motion, in the airborne case, this information is not always available from inertial navigation unit. Sometimes it must be recovered from the radar signal itself using the techniques known as autofocus. One of the critical parameters that can be retrieved is the ground speed, which is biased by the inertial navigation unit drifts and to which SAR processing is extremely sensitive. The ground speed can also be recovered from differential GPS technique, but this would require a cooperative GPS receiver on the ground.

There are two broad classes of autofocusing algorithms:

–those tracking the phase of pointwise reflectors (Phase Gradient Algorithm) or measuring the Doppler frequency bandwidth (Power Spectrum Analysis),

–those measuring the geometrical displacement between separate looks or the defocusing blur (Map-Drift, Reflectivity Displacement Method, Complex Correlation in Frequency Domain).

The algorithms in the first class have the advantage of correcting any type of trajectory error on the vicinity of a bright pointwise reflector. Those in the second class have the advantage of not relying on the existence of a pointwise reflector.

The map-drift technique uses the comparison of looks corresponding to different squint angles, in order to derive a velocity bias on the trajectory measurement and calculate the image using a corrected trajectory. Since the look distortion corresponding to possible trajectory errors, (even a constant velocity error) is nonlinear in nature, a simple linear correlation between the looks is not a solution. The classical map-drift algorithm, for example, uses a limited radial distance subrange contening the highest reflectors, therefore limiting the distortion nonlinearity along the radial axis.

This paper describes an original method designed at ONERA for the registration of looks. It improves the map-drift autofocusing technique by making it time variant thus allowing for the correction of low frequency trajectory errors, and not only velocity bias. The proposed algorithm considers that locally on a little patch of each look, the distorsion can be approximated by a translation. Thus under a given hypothesis on trajectory errors, we can obtain a good measure of the matching of the looks by the sum of the local (linear) correlations on a sampling grid on the common part of the two looks.

For the sake of computational efficiency, correlation around its maximum is approximated by a quadratic thresholded function. The trajectory errors are modelled by a Fourier-like sum of basis functions, of which the coefficients are estimated by a non-linear optimisation of the matching measure.

In order to reduce the cost of local correlation computations, a multi-scale "coarse to fine" approach may be used to decrease the number of computation points for the correlation on the patch.

For those not familiar with Synthetic Apeture Radar (SAR) imaging technique, Section 2 below recalls briefly the basic concepts. Section 3 describes the adaptive preintegration technique employed while processing the image, and its consequences on the image quality. The fourth section addresses the map-drift autofocusing method. Some applications to focus on a ground moving target and to registration are mentionned in Section 5.

The signal used was recorded on the RAMSES radar designed and operated by ONERA[6]. This modular experimental radar can accommodate up to four units simultaneously. It is versatile and has been used in many configurations as: ISAR for imaging airplanes from the ground, SAR or beam scanned radar on an airplane and for ground to ground surveillance. It also includes an optical and an infrared (3-5µ) camera. Signal is generally recorded and processed off line, to allow research on processing algorithms. The radar was operated in the deramp and in the frequency agility modes.

All the illustrations of this paper come from one flight (primarily intended to moving target imaging) for which the radar was populated with two units, one in the Ku and another one in the X band. Chirp pulses (of 110MHz bandwidth) emitted at a PRF (pulse repetition frequency) of 12,5kHz were deramped with a frequency shifted replica and sampled at a rate of 30MHz. Three successive ramps were then preintegrated before recording, thus yielding an apparent PRF of 4170Hz. Imaging distance was about 5500m, for an antenna aperture of about 12°. The airplane, flying at about 80m/s was subject to a lateral wind drift of 9° thus allowing imaging with a squint from 0° to about 15°.

2. BASIC CONCEPTS OF SAR IMAGING

The conceptual principle of a radar is to remotely detect and range, a radio-wave reflecting object by sending an electromagnetic pulse in a narrow beam and measuring the time elapsed before the reception of an echo. An image of an area may be obtained by steering the antenna —the popular parabolic dish— in several directions in space (e.g. rotating all around the horizon).

This image is only conceptual, since an accurate measure of the pulse fly-time requires very short pulses and since we must wait for the echo to be received before emitting the next pulse (e.g. 18 µs if the observing range is 5 km) the instantaneous power is extremely high with respect to the average power required.

The range pulse compression technique solves this problem spreading in time the pulse energy by differently delaying the frequencies of the pulse before amplification and performing the converse operation after reception of the echo. For example, in imaging *(fig. 1)*, the RAMSES radar emitted a 2 km long chirp (impulsion spread as a linear frequency ramp) of which the power is only 20 W, but is equivalent to a 13 m long pulse of 180 kW.

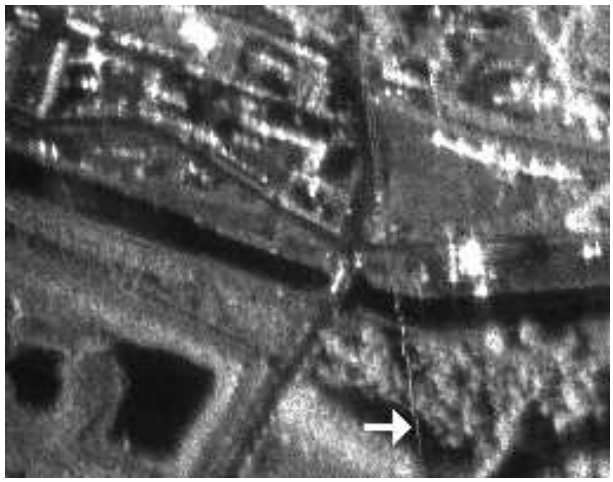

Fig. 1 – 2Hook image (arrow designates a moving traget)

The recompression of the received echo involves the modulation with a similar chirp (the replica) and a Fourier transform. In the RAMSES radar, the demodulation is done analogically before the digitising of the signal, hence called deramped signal.

The second difficulty is that diffraction limits the directionality of the emitted beam to an amount inversely proportional to the antenna size. This explains the huge dimensions of remote watching radars or radio-telescope aerials, and dramatically limits the angular resolution of an

airborne, hence small sized, radar. For example, the raw angular resolution of the RAMSES antenna used for *(fig. 1)* corresponds to 600 m on the ground.

The synthetic aperture technique solves this problem exploiting the motion of the aircraft for computing the echoes from an highly directive "virtual" antenna by combining recorded echoes from successive pulses. The principle is that a given point on the ground remains in the raw beam during 600 m of the flight *(fig. 2)*(a), hence we can sum the echoes, recorded with phase and amplitude during an integration time, and simulate a long and narrow receiving antenna. The computation of a synthetic antenna focused to a target point requires to change the relative phase of the different pulse echoes in such a way to emulate a constant optical path length between the target point and each of the successive real antenna position. Thus, a synthetic antenna corresponding to a given stretch of the trajectory may be steered in squint angle by adjusting the phase changes. Since the real trajectory is close to a uniform linear motion, the nominal trajectory, the phase change is nearly proportional to time, the proportion factor is called the Doppler frequency corresponding to the squint angle.

It is possible to compute a long panoramic image by stacking the range processed echoes provided by a sliding synthetic antenna operating at a constant squint angle. Each line of the panoramic image corresponds on the ground to the intersection between the ground plane and the cone of given squint angle, thus a piece of hyperbola. Generally, the synthetic antenna is shorter than the illumination time, see *(fig. 2)*(b), thus allowing to compute as in *(fig. 2)*(c), several images called looks with several squint angle values. The image on *(fig. 1)*, for example, is the sum of 21 looks computed with successive 70 m long synthetic antennas.

Since aircraft cannot fly along a straight line with a speed exactly uniform, the synthetic antenna formula (i.e. the phase changes between pulses) varies with time, and a given squint angle relative to the nominal trajectory *(fig. 2)*(a) does not correspond to the angle between the true trajectory and the observed direction, nor to a constant Doppler frequency. It is thus also possible to compute an image for a constant Doppler frequency or a constant real instantaneous squint, but its lines would not be evenly spaced nor evenly oriented on the ground.

The motion compensation is the way one deals with the variation in time of the synthetic antenna formula.

Autofocus designates techniques using the radar signal itself in order to infer, or improve the accuracy of the mismatch between the real and the nominal trajectories.

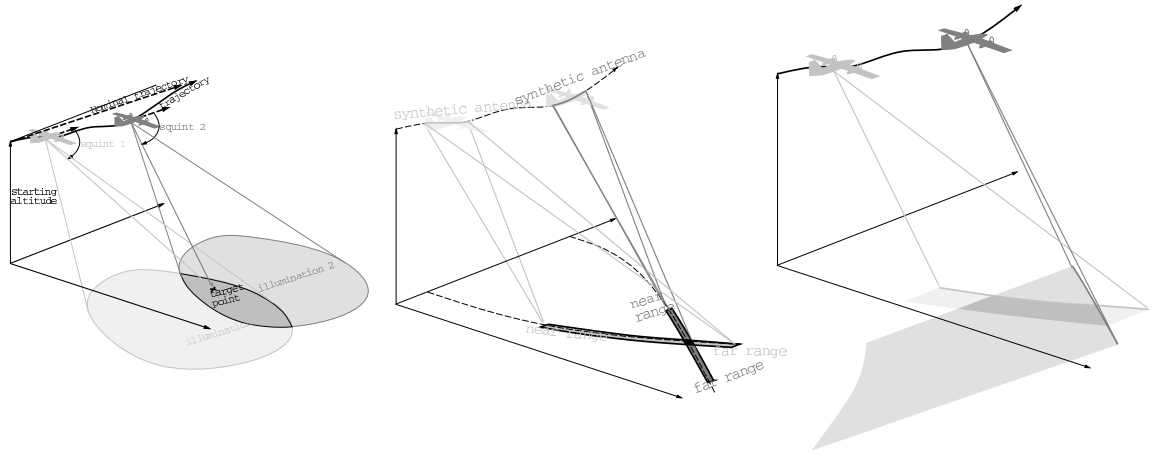

Fig. 2 – (a) Geometry of the airborne Synthetic Aperture Radar. (b) Example of two synthetic antennas operating at different squint angles. (c) How two sliding synthetic antennas operating at different constant squint angles produce two looks.

3. ADAPTIVE PRE-INTEGRATION

Compared with a satellite, an aircraft (and especially a light unmanned one) has a relatively jerky trajectory that cannot be assimilated to a straight line as soon as the expected ground resolution is in the range of tens of meters. The consequence is that the image is not directly superposable on other images obtained by the same sensor at a subsequent time within the same flight over. The magnitude of the distortions is much higher than the distance between the nominal (linear or assumed) trajectory and the effective trajectory. For example a non uniformity of the speed along a linear trajectory induces variations of the real squint angle with respect to the nominal squint angle that are proportional to the speed fluctuation. Minute fluctuations arising between the integration times for two different looks on the same point on the ground, amplified by a huge lever of the sensor to ground distance may easily result in a large mismatch between the looks.

Conversely, the measurement of this mismatch provides information of the unmodelled motion fluctuations. This is the very principle of the autofocus technique described here.

The images on *(fig.3)* and *(fig. 4)* show an example of the same radar data processed assuming a uniform linear trajectory, and processed using trajectory measures from inertial navigation unit(1). The inertial trajectory is not far from linear: During the 45 seconds of data recording, vertical deviation are within ±0.6m and horizontal deviations are within ±10m (for a total path of 3600m). Speed along track fluctuates of ±0.4m/s (for a speed of 80m/s). It means that the trajectory is linear with a precision better than 0.5% !

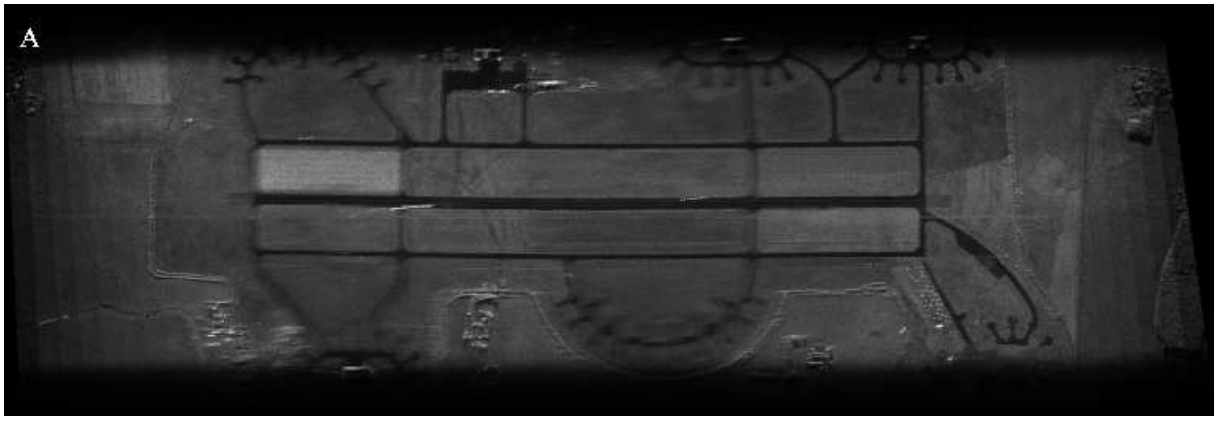

Fig. 3 – 9 look images (950Hz Doppler width, 2cm wavelength), altitude 2500m, range 5500m, swath 800m, without motion nonlinearities compensation. Note that the motion blur is not homogeneous

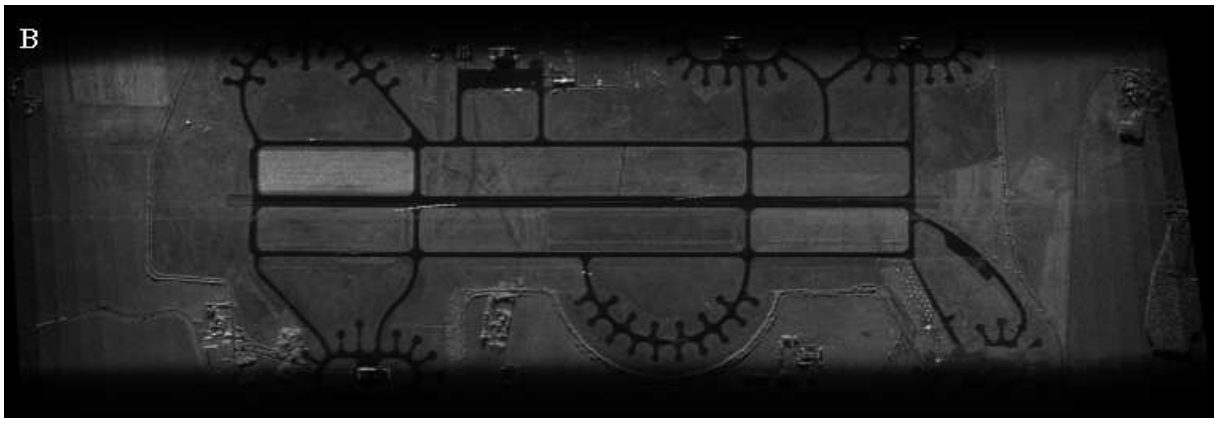

Fig. 4 – 9 look images with motion nonlinearities compensation. Effect on image sharpness is drastic although motion nonlinearities do not exceed 0.5%.

Assuming the motion of the centre of phase of the antenna is known with enough accuracy, it is extremely easy to take into account the nonlinearities of the trajectory provided azimuth compression is done in the time domain. The point response replica is simply computed from the distances between the centre of phase of the antenna and the focus point on the ground. The constraint of processing in the time domain, however, has an high price in computer power required (since it amounts to replace an FFT-based correlation with a direct correlation(2)) It also has its price in image quality since range migration is doneby sampling or interpolating the range-compressed pulses according to the distance of the focus point.

(1) As a matter of fact, both processings use a ground speed corrected for INU drifts by the autofocus technique described thereafter. Differential GPS may also be employed for providing the necessary drift compensation.

(2) If N is the number of pulses within the integration time, and L the number of independent looks within the Doppler ambiguity range (i.e. the number of radar pulses during one azimuth pixel, or the ratio between azimuth resolution and real antenna aperture) the comparison is roughly between an N-sized FFT and inverse-FFT and $\frac{N^2}{L}$ *multiplications. In the airborne example of (fig. 4) N≈2200 and L≈70, whereas in space-borne cases L is typically a few units.*

Range migration by sampling introduces an aliasing noise that results in a loss of image sharpness and range migration by interpolation (e.g. by 0-padding before range-compression) increases both memory and computing power requirements. Correlation of the raw signal with a full two-dimensional replica allows a proper treatment of the range-migration problem[4], since translation maps to a constant frequency modulation in the spectral domain. Its use, however, is limited to linear (circular in the space-borne case) trajectory since the replica should be constant within the time span of the FFT.

Pre-integration is simply an early processing along the Doppler axis. It combines pulse responses from a few successive ramps with an adequate complex weighting such as to simulate a small synthetic antenna with a narrower beam at receiving. It may be interesting for reducing the computation workload in the case the PRF is higher than the desired pixel spacing along track (this means that the illumination beam is wider than what is strictly needed for the resolution to be reached, a frequent situation in airborne SAR imaging).

The main benefits of this preprocessing, here, is that the velocity of the center of phase of the small synthetic antenna (denoted *n* on *(fig.5)*) can be made constant by varying the number of pre-integrated samples P_i, while tuning the small synthetic antenna P_1-P_n, which is moderately directive, in a constant squint direction *n-T*.

So to speak the signal is "resampled" to a linear uniform trajectory.

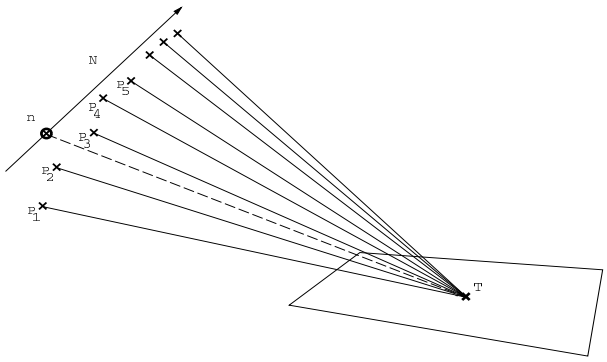

Fig.5 – Principle of adapted pre-integration, raw signal corresponding to pulses recorded at real position P_1, P_2... are summed for focusing target point T in the middle of the swath with center of phase n on the nominal trajectory N.

The first two looks are computed from the signal pre-integrated assuming the measured trajectory for two widely separated squint angles. Due to the nominally linear uniform motion, this processing may use two dimensionnal as well as time domain processing.

The autofocus procedure will compute trajectory corrections from the geometrical mismatches between the two looks. The correction will be feed back to the motion compensation and the SAR processor.

For the sake of computational efficiency, the loop is first done with a low resolution while the error bounds are large, and then a second iteration is done with full resolution and smaller error bounds.

4. MAP-DRIFT AUTOFOCUSING USING LOCAL CORRELATION

Most autofocus algorithms may be gathered in two broad classes: those tracking the phase of point-wise reflectors such as PGA (Phase Gradient Algorithms) [10] or measuring the Doppler frequency bandwidth such as the PSA (Power Spectrum Analysis) on one side, and on the other side those measuring the geometrical distortion between separate looks or the defocusing blur (contrast optimization). Algorithms of the second kind, such as Map-Drift, RDM (Reflectivity Displacement Method) [11] or less efficient CAFE (complex correlation in frequency domain), are generally preferred since they do not rely on the availability of bright point-wise reflectors.

The map-drift technique uses the comparison of looks computed with different squint angles (or Doppler frequencies) to derive low frequency errors in the trajectory measurements. These low frequency errors once identified are used to correct the trajectory and the final image is synthesized with the corrected trajectory.

It has been suggested [11] to reiterate the process with shorter integration times for retrieving higher frequency motion errors. But decreasing integration times, diminishes azimuth resolution, thus the accuracy of the look matching, therefore introducing high frequency noise in the reconstructed trajectory.

One of the most common trajectory measure error is a bias on the ground velocity due to drifts of the aircraft navigation system. An other one is a misalignment and/or lever errors between the inertial navigation unit (INU) of the aircraft and the radar antenna (yielding unmodeled errors in the 1Hz frequency range).

Even if the errors are simple (e.g. a constant velocity error), the induced distortion effect on the several look images are generally not linear, the reason is that the swath length is not negligible with respect to the range (around 1/4 in our example), hence the squint error introduced by velocity errors varies within the swath, furthermore the nonlinearity of the airplane trajectory results in nonlinearities of the distortions effects.

For making the computation feasible, we simplified the trajectory errors expanding them into a Fourier like sum of one linear and a few sinusoidal error terms, as illustrated on *(fig. 6)*, or any appropriate function set. The goal is then to estimate a now reduced set of error parameters.

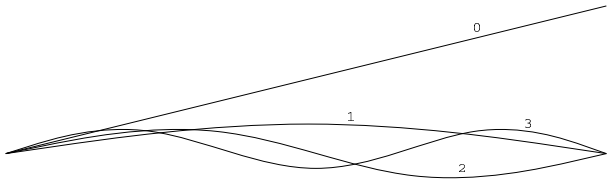

Fig.6 – First 4 basis error functions for trajectory correction (e.g. on North-South axis)

One should bear in mind the fact that the error parameter estimation problem is still highly nonlinear since, although the trajectory error is now defined as a linear combination of a basis of error functions, the effects of the trajectory error on different looks distortion is nonlinear in nature. We must use an iterative algorithm for nonlinear maximization of the correlation of the "distortion corrected" looks. The computational burden for evaluating the correlation function at one point in the parameter space is hence extremely critical. This was solved by assuming that, locally, distortion is closely approximated by a translation.

The algorithm [12], [13] takes a rectangular sampling grid on the intersection of two looks (computed at two extremities of the illuminating beam) and takes, around each node of the grid, small rectangular patches of one look skewed to the geometry of the other look (with the initial guess of the parameters). For each skewed patch, a correlation function is computed within a neighborhood of the corresponding position (for the initial guess of the parameters). This local correlation function is then used to compute a quadratic cost function, to be maximized in the optimization process.

The correlation used is the "true" correlation (that is the ratio of the cross-variance to the product of the standard deviations). This is definitely not the result of the FFT-based "fast correlation" algorithms. Since even a moderate velocity bias may be amplified by the squint lever to a large geometrical mismatche between the looks, the cost for the computation of the correlation (proportionnal to both the number of pixels of the patch and the rectangle of tested translations) increases as the 4^{th} power of the resolution. This explains why it is much more efficient to make the first autofocus loop at lower resolution. It is furthermore of little use to start at the full attainable resolution, since the images is, by definition, slightly out-of-focus at the first try.

The quadratic function is centered on the correlation minimum, with a matrix corresponding to inertial matrix of a neighborhood of the correlation function. To avoid biases caused by clear mismatches of the correlation of some patches, the quadratic function is bounded above at a level proportional to the correlation maximum value.

Using the inertial matrix ensures that if there is ambiguity in matching in one direction, the local contribution to the cost function will be neutral along that direction. Part *A* of *(fig. 7)* illustrates the case when the correlation is non ambiguous, from left to right we have the skewed patch from look1, the neighborhood from look2 around the corresponding spot (for the initial guess of parameters), the local correlation mapping, with scale from white=1 to black=0 and below, and the cost function. Part *B* of *(fig. 7)* illustrates the case when the correlation is ambiguous. It is on this image difficult to localize the small patch along the boundary between the two different ground use, but its location across the boundary is very accurate.

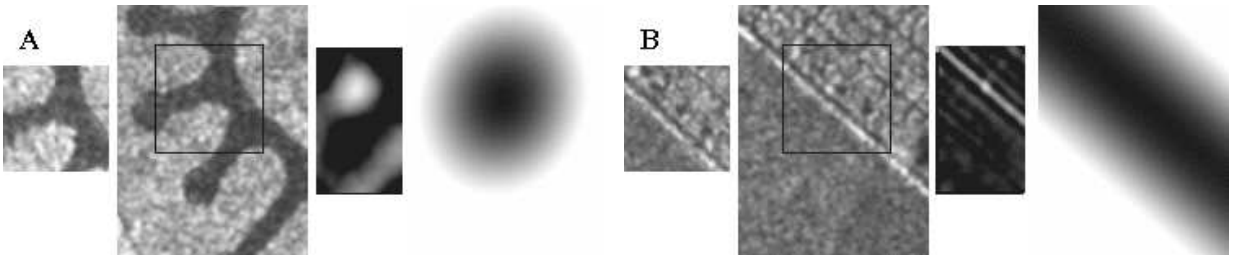

Fig.7 – Look 2 skewed to look 1 geometry, neighborhood in look 1, correlation function and cost function: A generic case B degenerate (ambiguous) case.

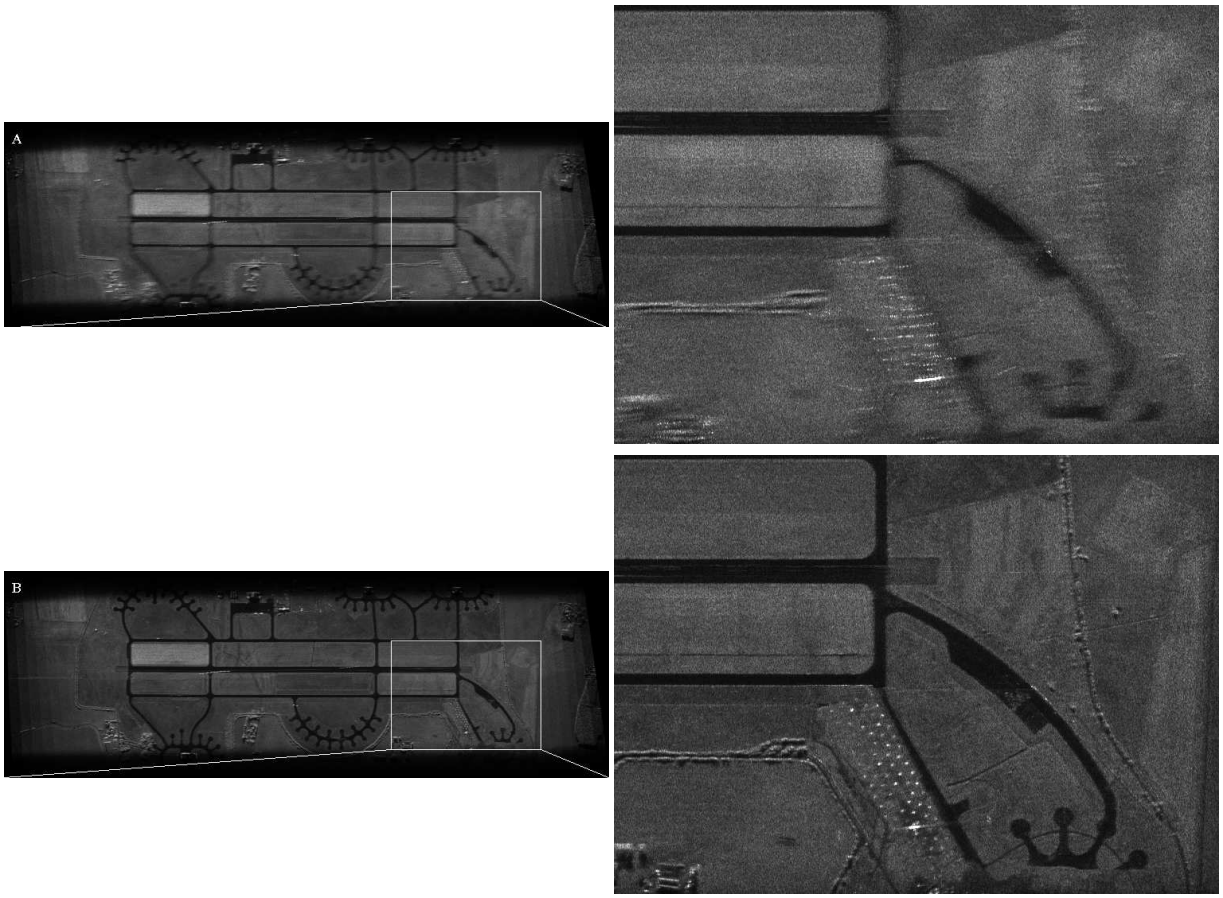

Fig.8 – 9look image at a pixel size of 13m: A focused with raw INU data. B refocused with autofocus.

The optimization of the matching of the two looks is then performed by a crude multidimensional optimization procedure (downhill simplex) with a cost function obtained by computing the registration with the candidate parameters of the centers of each patch (between both looks) and summing the partial cost function corresponding to the mismatch within each patch.

The process is much more efficient than directly computing the correlation between the looks since we replace the computation of the registration of, for example, 4000x1000 pixels by the registration of a mere 100 patch centers.

In *(fig. 8)* is illustrated an example of such an autofocusing technique with data obtained on the same flight. The algorithm was used for correcting an altitude bias (bounded at 100m), an horizontal velocity drift (bounded at 2m/s), a vertical slope bias (bounded at 0.3m/s) and a lever from the INU to the center of phase of the antenna. Part *A* of *(fig. 8)* is the image resulting from a computation with a blind trust of the INU data. Part *B* shows the image obtained after refocusing with a velocity increase of 1.6m/s (within the accuracy tolerances for a 1nm/h rated INU) a drift angle increase of 1.5° and a lever of 24cm along track, 43cm across track and 1m vertically.

5. AUTOFOCUS DERIVED APPLICATIONS

There are cases where successive looks do not match locally because during the small time lapse separating their acquisition, something has moved within the patch. This is known as the "moving target indication" (MTI) problem. One could think that measuring the displacement of a point target between several looks (assuming a uniform linear proper motion for the target) allows to compute target position and velocity. A careful analysis[14 15] shows that this is not the case. There is a remaining degree of freedom, which is the across track component of the vehicle proper velocity.

This may seem surprising since some autofocus techniques, such as PGA, use the tracking of a single point-like reflector to focus the image ! However, the across-component of the velocity is not needed to focus on the target (it is the very reason why it cannot be derived from the apparent position change). In fact, an error in this parameter is linked to an error in the effective squint angle estimation. Thus, in the extreme case of a perfectly linear uniform aircraft trajectory, a bias in this parameter will leave the image unchanged in the slant-time coordinates. The "ground coordinate conformed image" would, howerver, be skewed with respect to the correct image.

Though, in the moving target case, the effective squint angle can be evaluated from comparison between the variation with Doppler frequency of the backscattering of the target and that of the background, its accurate determination requires extra hardware for having a true resolution capability in squint angle.

The technical solution implemented is generally to have a two-port antenna, that is the real antenna is split into two sub-antennas having beam-width similar in shape but slightly shifted. After all the target focusing process is done, one only need to cancel the target by adjusting a phase delay between the two sub-antennas to obtain an accurate estimation of the squint angle, hence of the remaining parameter [16]. This technique is similar to the single-pulse tracking radar technique using sum and difference antenna patterns for ground to air application. It is well known that this technique requires a maximum rejection of the clutter. That is precisely what the SAR imaging and plot tracking processes do. It is obvious that in air to ground configuration without SAR processing, the targets are completely hidden by the reflections from the landscape. Alternative hardware solutions for cancelling the background have been implemented [17], but this requires continuous adaption of the pulse repetition rate in order to match the horizontal separation of sub-antennas and the aircraft motion between successive pulses.

Target tracking, at least for the three degrees of freedom of the horizontal motion accessible to picture processing, results in a further increase in target to background contrast because the background is incoherently summed whereas the target is coherently summed between the looks. On the view of *(fig. 8)* there were two vehicles running (with known velocity) along the runway, *(fig. 9)* shows different focusings on one of the two targets. Part *A* of *(fig. 9)* is the middle look from the 9 used, part *B* is a zoom on the 9-look image of *(fig. 8)*, part *C* is the middle look once focused on the target (with the proper velocity parameters computed from tracking) and part *D* of *(fig. 9)* shows the 9-look image focused on the target. In fact, for this last image (part *D*), the "true" target velocity was 55 km/h along the track, but we focused the image with an "equivalent" velocity of 100 km/h and a direction at about 50° from the track axis. This shows well that the focusing on the target does not depend of its across track velocity component.

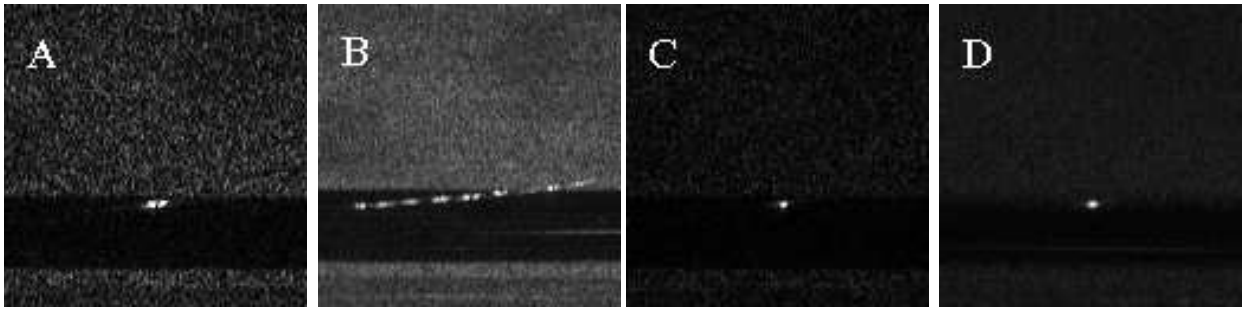

Fig. 9 – Focusing on a moving target (images are normalized to the maximum amplitude on the target, the background seems lighter as the target peak amplitude grows larger): A middle look focused on the ground. B 9-look image focused on the ground. C middle look focused on the target. D 9-look image focused on the target.

The autofocusing algorithm described above, however, is not simply equivalent to focusing point-wise targets all moving with the same velocity (the opposite of the aircraft velocity bias). For the purpose of autofocusing, the velocity fluctuations of the aircraft provide the missing across track component of its own velocity bias. The reason is that the squint *versus* across-track component ambiguity changes with the along track

velocity. Thus an incorrect hypothesis on the effective squint angle will result in a non constant skewing of the looks along the whole image if the aircraft velocity varies. The skew error is not the same for the different looks since their acquisition is separated by seconds. On a point, it is possible to match them by making an error on the along track velocity, but globally (on the whole image) it is impossible to match them if there remains an across track velocity bias.

This is one of the advantage of global methods for autofocus, compared to local methods as PGA.

The image matching technique used for autofocus may also be used for matching images from successive overlapping views over some area. It is necessary to register the images because navigation drifts from one view to another result in large positioning error. Though the transformation from one image to another is here simply a translation, the local correlation technique is still useful because bright points may fluctuate in backscattering from view to view thus jeopardizing the usability of crude image correlation (furthermore images are non stationary in nature). *(fig. 10)* shows an application of this technique on three views taken with heading separated from 45° and 90°, illustrating the robustness of the approach (matching was made at three successive scales to lower computational workload).

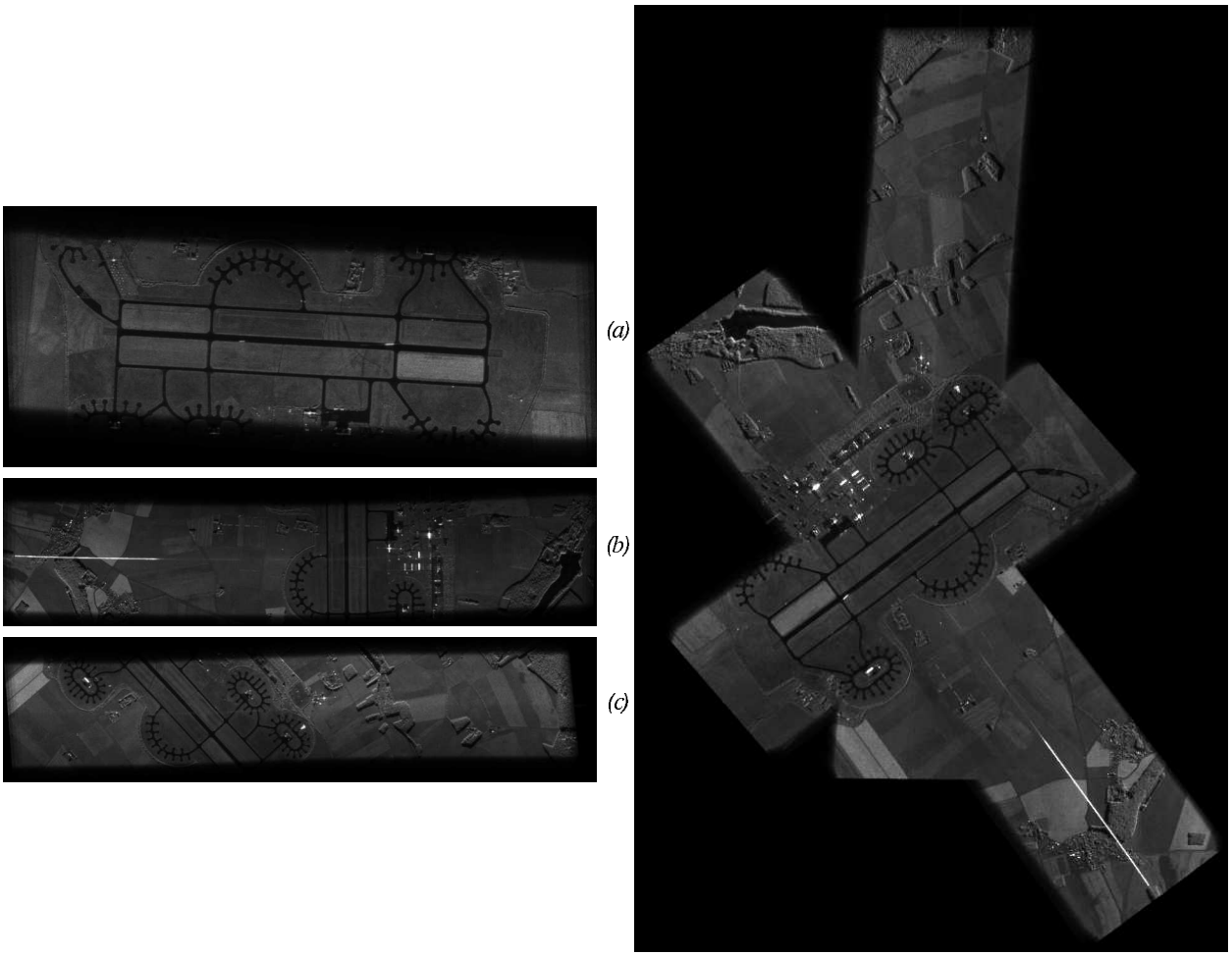

Fig. 10 – Example of matching of successive views using local correlation technique: (a) (b) (c) three different views, (d) composite view.

6. CONCLUSION

Compared to the high regularity and predictability of spacecraft trajectories, aircraft motions are much more irregular and difficult to measure accurately.

An original method designed for the registration of looks has provided a time variant map-drift autofocusing technique. This has also been adapted to detect moving objects or to match separately acquired images for making mosaic images.

Feasibility and efficiency of the proposed algorithm have been validated on real airborne SAR signals acquired on several wavelength and geometrical conditions.

7. REFERENCES

1 Franceschetti G., Schirinzi G.– A SAR processor based on two-dimensional FFT codes, IEEE trans. on Aerospace & Electronic syst. 26-2 p.356-365 March 1990.

2 Raney R.K.– An exact wide field digital imaging algorithm, Int. J. Remote Sensing. 13-5 p.991-998 March 1992.

3 Balmer R., Runge H.– A novel high precision SAR focusing algorithm based on chirp scaling, proc. IGARSS 92 Houston USA 1992.

4 Massonnet D., Adragna F., Rossi M. CNES general-purpose SAR correlator IEEE trans. Geosc. & Remote sens. Vol 32, p.636–643 (1994)

5 Büdenbender H.– Aufbau eines zweidimensionalen SAR-Prozessors für flugzeuggetragene SAR-Systeme, Deutsche Forschungsanstalt für Luft- und Raumfahrt DLR-FB 93–40 Oberpfaffenhofen 1993.

6 Duplex N., Boutry J.M.– Étude de performances SETHI, ONERA technical report, 1/7268/SY Châtillon, France, November 1994.

7 Bierens L.– Feasibility study of an on-board high resolution real-time airborne SAR processor, proc. microwave 94 conf. p.68-73 London 25-27 October 1994.

8 Cantalloube H.– Synthèse d'images SAR à partir des données brutes, ONERA technical report 1/3775.SN Châtillon, France, July 1995.

9 Cantalloube H., Nahum C.– Nouvelles fonctions du logiciel de démonstration ramsesXII, ONERA technical report 2/3775.SN Châtillon, France, May 1996.

10 Wahl D., Jakowatz C., Thompson P., Ghiglia D.– New approach to strip-map SAR autofocus, Sandia National Labs CONF 9410901-1 SAND 94-1175C Albuquerque, USA, 1994.

11 Belcher D., Horne A., Baker C.– Algorithms for focused spotlight mode SAR imaging, proc. microwave 94 conf. p.74–81 London 25-27 October 1994.

12 Duplaquet M.L., Cantalloube H.– Une méthode globale de recalage inter-images, 14ème colloque GRETSI Juan-les-Pins, France, September 1993.

13 Cantalloube H., Nahum C.– Autofocusing of (inverse) synthetic aperture radar for motion compensation, NEACON 96 proc. Dayton, USA, May 1996.

14 Sicard D.– SAR MTI with wide beam antenna, Piers Symposium, Seattle, July 1995.

15 Cantalloube H., Nahum C.– Détection de cibles mobiles par imagerie multivues, ONERA technical report 3/3775.SN Châtillon, France, May 1996.

16 Ender J.– Signal processing for multi-channel SAR applied to the experimental SAR system AER, proc. Int. Conf. on Radar 94 p.220-225 Paris, France 3–6 May 1994.

17 Barker D., Baker C.J., Horne A.M., Currie A., Edwards R., Warren K.– C band SAR, proc. microwave 94 conf. p.53–61 London 25-27 October 1994.

Biography :Carole NAHUM was born in 1960 in Tunisia. She joined the Ecole Nationale Supérieure des Télécommunications in 1982 (Paris). She obtained her PhD in Mathematics from McGill University, Canada in 1988. Since then, she has been working as a scientist at the Office National d'Études et de Recherches Aérospatiales in France (National Air & Space research Directorate). She is now leading researches in SAR signal processing and interferometry for air and space military applications.